Received: 10 July 2023 | Revised: 22 September 2023 | Accepted: 6 October 2023

DOI: 10.1111/gcb.16999

Global Change Biology WILEY

RESEARCH ARTICLE

Peatland pools are tightly coupled to the contemporary carbon cycle

Joshua F. Dean[1] | Michael F. Billett[2] | T. Edward Turner[3,4] | Mark H. Garnett[5] | Roxane Andersen[6] | Rebecca M. McKenzie[7] | Kerry J. Dinsmore[7] | Andy J. Baird[3] | Pippa J. Chapman[3] | Joseph Holden[3]

[1]School of Geographical Sciences, University of Bristol, Bristol, UK

[2]Biological and Environmental Sciences, University of Stirling, Stirling, UK

[3]water@leeds, School of Geography, University of Leeds, Leeds, UK

[4]Forestry and Land Scotland, Dumfries, UK

[5]National Environmental Isotope Facility Radiocarbon Laboratory, East Kilbride, UK

[6]Environmental Research Institute, University of the Highlands and Islands, Thurso, UK

[7]UK Centre for Ecology and Hydrology, Penicuik, UK

Correspondence
Joshua F. Dean, School of Geographical Sciences, University of Bristol, Bristol, UK.
Email: josh.dean@bristol.ac.uk

Funding information
Natural Environment Research Council, Grant/Award Number: NE/J007609/1 and NE/V009001/1; UK Research and Innovation, Grant/Award Number: MR/V025082/1

Abstract

Peatlands are globally important stores of soil carbon (C) formed over millennial timescales but are at risk of destabilization by human and climate disturbance. Pools are ubiquitous features of many peatlands and can contain very high concentrations of C mobilized in dissolved and particulate organic form and as the greenhouses gases carbon dioxide (CO_2) and methane (CH_4). The radiocarbon content (^{14}C) of these aquatic C forms tells us whether pool C is generated by contemporary primary production or from destabilized C released from deep peat layers where it was previously stored for millennia. We present novel ^{14}C and stable C ($\delta^{13}C$) isotope data from 97 aquatic samples across six peatland pool locations in the United Kingdom with a focus on dissolved and particulate organic C and dissolved CO_2. Our observations cover two distinct pool types: natural peatland pools and those formed by ditch blocking efforts to rewet peatlands (restoration pools). The pools were dominated by contemporary C, with the majority of C (~50%–75%) in all forms being younger than 300 years old. Both pool types readily transform and decompose organic C in the water column and emit CO_2 to the atmosphere, though mixing with the atmosphere and subsequent CO_2 emissions was more evident in natural pools. Our results show little evidence of destabilization of deep, old C in natural or restoration pools, despite the presence of substantial millennial-aged C in the surrounding peat. One possible exception is CH_4 ebullition (bubbling), with our observations showing that millennial-aged C can be emitted from peatland pools via this pathway. Our results suggest that restoration pools formed by ditch blocking are effective at preventing the release of deep, old C from rewetted peatlands via aquatic export.

KEYWORDS
carbon dioxide (CO_2), dissolved organic carbon (DOC), methane (CH_4), particulate organic carbon (POC), peatlands, pools/ponds, radiocarbon (^{14}C), stable carbon isotope ($\delta^{13}C$)

1 | INTRODUCTION

Peatlands are important long-term terrestrial carbon (C) stores. They cover only ~3% of the Earth's land surface yet contain 600–650 Pg C fixed into peat soils from the atmosphere by primary production and maintained for millennia under water-logged conditions (Page et al., 2022; Xu et al., 2018). The magnitude of this C store is comparable to that currently held in the atmosphere (875 Pg C; Friedlingstein et al., 2022). Peatlands release some C laterally to standing and flowing inland waters (i.e., streams and lakes; Dean et al., 2020), as well as emitting carbon dioxide (CO_2) and methane (CH_4) to the atmosphere (Evans et al., 2021), but under pristine conditions are net C sinks. However, peatlands are at severe risk of destabilization which could release the C they store to the atmosphere and aquatic systems (Lupascu et al., 2020). Climate change and changes in land use may cause the release of additional C that would otherwise have remained in peat soils. This additional C release comes from perturbation of contemporary C cycling and/or the release of millennial aged C that was previously held in deeper peat layers (Moore et al., 2013; Tanentzap et al., 2021).

Pools, or ponds, are small shallow standing water bodies that are commonly found in peatlands worldwide (Arsenault et al., 2022; Hassan et al., 2023). Ranging from <1 to 1000 m^2 in size and up to ~1 m in depth, pools can be hotspots of terrestrial C decomposition and CO_2 and CH_4 emissions, and provide a direct and rapid pathway for the release of C to the atmosphere (Downing, 2010; Holgerson & Raymond, 2016; Peacock et al., 2021; Rosentreter et al., 2021; Turner et al., 2016). Peatland pools are sensitive to both climate and land use change and could potentially serve as sentinels for shifts in patterns of peatland C cycling (Arsenault et al., 2023; Hassan et al., 2023).

Radiocarbon (^{14}C) is a powerful tool for detecting the age of C released from soils (Estop-Aragonés et al., 2020; Schwab et al., 2020; Stuart et al., 2023; Waldron et al., 2019). Inland waters integrate ^{14}C signals of the air, plants, and soil that mobilized C has moved through prior to its release. Recent advances have enabled sampling of all major C forms found in inland waters: dissolved and particulate organic C (DOC and POC, respectively), dissolved CO_2 and CH_4, and ebullition (bubble release from aquatic sediments; Dean et al., 2020; Prėskienis et al., 2021). For example, inland waters have shown clear signs of old soil C release from enhanced seasonal thaw of permafrost soils in Arctic catchments (e.g., Schwab et al., 2020) and artificially drained tropical peatlands (e.g., Moore et al., 2013). Often, ^{14}C markers associated with disturbance can be hidden within the larger signal of contemporary C turnover (Dean et al., 2019). In these cases, age distribution modelling can provide estimates of the likely contributions of different soil C layers to the mixture of C sources found in a single inland water ^{14}C sample (Dean, van der Velde, et al., 2018; Evans et al., 2014, 2022; Raymond et al., 2007; Tanentzap et al., 2021).

Many peatlands worldwide have been drained historically for agriculture or peat extraction, and these activities continue in some regions today (Evans et al., 2021). Heavily drained peatlands can release C that is ~1000–4000 years old into drainage waters (Hulatt et al., 2014; Moore et al., 2013; Waldron et al., 2019). In many regions, including Europe, Canada, and Indonesia, peatlands are being restored by blocking drainage ditches in an attempt to raise the water table, thereby reducing C loss to the atmosphere and aquatic systems (Evans et al., 2021; Parry et al., 2014; Putra et al., 2021; Waldron et al., 2019). Ditch blocking often results in the establishment of pools behind small dams (Chapman et al., 2022; Holden et al., 2018). These "restoration" pools may retain C that would otherwise be directly lost from peatlands via runoff into drainage ditches (Gaffney et al., 2021; Parry et al., 2014). It is therefore important to know whether pools formed through restoration efforts are receiving and emitting old C destabilized by legacy drainage, in addition to the contemporary C turnover expected under raised water table conditions (Evans et al., 2021; Parry et al., 2014; Waldron et al., 2019). Given that pools are important sites of organic C decomposition and emissions of CO_2 and CH_4 within peatland landscapes, climate change and further anthropogenic landscape disturbance could readily impact the substantial fluxes of C released into and from peatland pools (Arsenault et al., 2023; Chapman et al., 2022; Turner et al., 2016). Understanding the role of peatland pools is crucial to quantifying current and future C cycling in peatlands, yet little is known about the source of pool C. Do pools only receive and decompose contemporary peatland C, or do they have the potential to process and emit additional old C from deeper peat layers?

Here, we present a set of ^{14}C and stable C isotope ($\delta^{13}C$) observations of DOC, POC, and dissolved CO_2 collected simultaneously from a Flow Country blanket peatland in the north of Scotland across three sampling campaigns in 2014 and 2015. These observations are augmented by snapshot sampling in six pool locations on blanket peatlands across the United Kingdom that focused on CO_2 and DOC but also included rare ebullition ^{14}C samples. Organic C has accumulated in the peat soils of our study locations and in the United Kingdom's blanket peatlands in general over the past 8000–10,000 years (Billett et al., 2010; Ratcliffe et al., 2018). We sought to determine the source and age of C in peatland pools to establish where this C comes from, to what degree these pools receive C from the surrounding peat and release it to the atmosphere, and whether C sources differ between natural and restoration pools. Specifically, we aimed to answer the following research questions:

1. What is the age (source) of C found in pools across a range of temperate blanket peatlands?
2. How does the age (source) of pool C vary between two distinct types of peatland pools (natural and restoration)?
3. What is the relationship between pool C isotopes and key peatland pool biogeochemical parameters?

To our knowledge, this is the first comprehensive study of the isotopic composition of peatland pool C. We hypothesized that pools contain mainly contemporary C but will display clear signs of old C release if peatland destabilization is occurring.

2 | MATERIALS AND METHODS

2.1 | Study locations

We carried out isotopic measurements in three distinct geographical regions of the United Kingdom: northern and southwest Scotland and Northern Ireland (Table 1). All the pool complexes were on ombrotrophic plateaux; all sampled pools were situated in the peat matrix, and thus, geologic C inputs to these pools are unlikely. The Cross Lochs, Loch Lier, and Munsary locations are in the Flow Country of northern Scotland, the largest blanket peatland complex in Europe (~4000 km^2). The Silver Flowe is a blanket peatland located in a glacial valley in Galloway, southwest Scotland. Slieveanorra is an upland raised bog in County Antrim, Northern Ireland. Garron Plateau is also in County Antrim and is one of the largest areas of near-natural upland blanket bog in Northern Ireland. Vegetation in the pools included both submerged and emergent vegetation, and can be broadly classified into aquatic *Sphagnum* (e.g., *S. cuspidatum* and *S. denticulatum*), *Eriophorum* (e.g., *E. angustifollium*), *Menyanthes* (e.g., *M. trifoliata*), and algae including cyanobacteria (Turner et al., 2016). All sites experience similar climate; natural pools, sampled across all locations, shared similar hydrological and geomorphological characteristics, and pool waters shared similar pH, dissolved oxygen (DO), DOC, and CO_2 contents (Turner et al., 2016).

Natural pools were sampled at all locations. Restoration pools created by drain blocking were only sampled at the Cross Lochs and Loch Lier locations (Table 1). For the studied pools across all locations, natural pools tended to be larger than restoration pools but had similar depths (Figure S1; Table S1). Natural pools tended to have longer water residence times than restoration pools, and this was consistent across pools at the Cross Lochs location where data were available (Holden et al., 2018). Ditch construction to drain the peatlands at Cross Lochs and Loch Lier occurred in the 1970s (exact dates unknown) and targeted areas where peat was naturally shallower and better drained. Ditch blocking for restoration purposes through rewetting by raising the water table took place in 1998 at Loch Lier and 2002 at Cross Lochs, approximately 16 and 12 years prior to our sampling campaigns, respectively.

2.2 | Pool sampling

The greatest sampling intensity was in the natural and restoration pool systems at Cross Lochs (Dean et al., 2023). Three natural and three restoration pools at this location were sampled in May 2014, November 2014, and September 2015. Additional pools at Cross Lochs were sampled a single time (Table S1; Dean et al., 2023). At Loch Lier, two natural and two restoration pools were sampled in November 2014 during the same campaign as the Cross Lochs sites. In September 2015, all locations were sampled except Loch Lier due to logistical constraints (Table S1; Figure S1c). Pools were sampled under the same conditions in each campaign as far as possible; timing of the sampling campaigns had no clear impact on the observed patterns of C isotopic composition (Figures S1 and S3). Ice cover, which was not present on any pools during sampling, is generally limited to surface freezing for a few days or weeks during the coldest parts of winter.

Pool water sampling for isotope analysis focused on DOC and dissolved CO_2. In many cases, POC levels and dissolved CH_4 concentrations were too low for sufficient material to be collected for ^{14}C analysis. Isotope sample collection followed Dean et al. (2020). Water samples were collected in 1 L glass bottles previously furnaced for 3 h at 450°C, and were kept in a cool box immediately following sampling then placed in a refrigerator at 4°C at the end of the day and stored there for the duration of the field campaign (up to 3 days). The water samples were then transported to the NERC Radiocarbon Facility in East Kilbride in a cool box (up to 1 day). Upon arrival at the facility, samples were placed in a refrigerator at 4°C. The water samples were filtered within the next 3 days using pre-ashed glass microfiber filters (GF/F 0.7 μm). Where enough material was present, POC samples were collected by combusting these GF/F filters (Dean et al., 2020). Previous work has

TABLE 1 Study site characteristics. See Table S1 for full sample details. Data from Turner et al. (2016).

Region	Meteorological averages (1981–2010)	Location	Elevation (m asl)	Pools sampled
Flow Country, N Scotland	Mean daily temperatures (MDT): Max = 11.7°C Min = 3.6°C	Cross Lochs	211	Total = 11 Natural = 6 Restoration = 5 (3 of each repeat sampled)
	Annual precipitation = 1196 mm	Loch Lier	185	Total = 4 Natural = 2 Restoration = 2
		Munsary	105	Total = 3 Natural = 3
SW Scotland	MDT max = 12.8°C MDT min = 5.8°C Annual precipitation = 1120 mm	Silver Flowe	280	Total = 3 Natural = 3
Northern Ireland	MDT max = 11.5°C MDT min = 5.7°C Annual precipitation = 1313 mm	Garron Plateau	307	Total = 3 Natural = 3
		Slieveanorra	337	Total = 3 Natural = 3

demonstrated that this treatment of samples has no significant impact on DOC isotopic composition (Gulliver et al., 2010). After collection on the filters, POC samples were refrigerated (4°C) until combustion. CO_2 samples were collected by degassing 3 L of sample water into a 1 L CO_2-free headspace for 3 min, and the headspace then injected onto a molecular sieve cartridge in the field (Garnett et al., 2016). We also include a single dissolved CH_4 sample collected from Loch Lier in November 2014 as part of a separate study (Dean et al., 2017).

Bubble traps were deployed to collect ebullition (bubble) samples from six natural and five restoration pools at Cross Lochs. Two to six traps were deployed in each of the larger natural pools, and one trap was deployed in the smaller restoration pools due to space constraints. The bubble traps comprised stoppered inverted glass funnels of inside diameter 246 mm (area = 0.0475 m^2). The funnels were kept on the pool surface by a circular "lifebuoy" type float made from pipe insulation. Funnels were filled with pool water which is drawn into the funnel by a large syringe via a three-way gas-tight valve. When deployed, rising bubbles displace the water in the funnel, allowing ebullition bubbles to accumulate. The traps were deployed on May 21, 2014 and checked fortnightly until collection on November 5, 2014. Ebullition samples were extracted from the funnel traps using a syringe purged of ambient air and injected into an N_2-flushed gas bag. Where multiple traps were deployed in a single pool, the bubbles from each trap were combined into a single sample. CO_2 was separated from CH_4 in the gas bags by filtering the gas sample through molecular sieve cartridges in the laboratory during sample processing (Garnett et al., 2011). Six samples yielded sufficient material for ^{14}C-CH_4 analysis (four from natural pools and two from restoration pools), and only one sample yielded enough for ^{14}C-CO_2 (natural pool; Table S2).

Sediment grab samples were collected from three pools at Cross Lochs, two natural pools and one restoration pool (Table S1). The top ~20 cm of pool floor sediment was collected using a simple corer and refrigerated at 4°C prior to analysis. Each pool sediment sample was cold acid washed (1 M HCl) overnight to remove carbonates, homogenized by stirring with a glass rod, freeze-dried, and then combusted to CO_2 for isotope analysis using the sealed quartz tube method (Boutton et al., 1983); glassware was cleaned by combusting at 450°C for at least 3 h.

2.3 | Isotopic analyses

The samples were processed at the United Kingdom's Natural Environment Research Council Radiocarbon Facility in East Kilbride, Scotland. The filtered DOC samples were rotary evaporated to solids. DOC solids and POC filters were acid fumigated to remove any inorganic C, then combusted to CO_2. POC samples were combusted using the standard Boutton et al. (1983) sealed quartz tube method which involves complete thermal oxidation of the organic matter; the POC and the filter were combusted together. Dissolved CO_2 samples were recovered from the molecular sieve cartridges by heating to 425°C (Garnett et al., 2019). The ebullition samples were first filtered through a molecular sieve cartridge to remove CO_2, and the CH_4 was then oxidized using a platinum bead catalyst at 950°C to CO_2. In one case, there was enough CO_2 in the ebullition sample for ^{14}C analysis as well. For all ^{14}C samples, the CO_2 produced was graphitized using Fe-Zn reduction. Where there was >1 mL CO_2, an aliquot was extracted for δ^{13}C analysis using a dual-inlet isotope ratio mass spectrometer (Thermo Fisher Delta V) and reported relative to the Vienna Pee Dee Belemnite (VPDB) standard. ^{14}C content was determined using accelerator mass spectrometry at the Scottish Universities Environmental Research Centre, East Kilbride. Where sample size was <0.5 mL CO_2, samples were analyzed at the Keck Carbon Cycle Accelerator Mass Spectrometer facility at the University of California Irvine. Following convention, ^{14}C content was normalized to a δ^{13}C value of −25‰ and presented as fraction modern carbon ($F^{14}C$); conventional radiocarbon ages were provided for samples with $F^{14}C$ content <1 in years before present (yBP) where "present" is defined as 1950 CE (Stuiver & Polach, 1977). Radiocarbon-dead and known-age standards were processed alongside the samples to quantify the ^{14}C background and verify the radiocarbon measurements, respectively. The ^{14}C-dead standards (bituminous and anthracite coal) quantified the extraneous C associated with the processing and were used to background correct the sample results using the method described by Donahue et al. (1990). Barley mash from the Third International Radiocarbon Intercomparison (Gulliksen & Scott, 1995) and an internal humin standard (96H humin; Xu et al., 2004) were used as radiocarbon reference standards to verify the accuracy and precision of the sample results.

2.4 | Statistical analyses

The aquatic samples we collected contain mixtures of C of different ages that contribute to a single "'bulk" $F^{14}C$ value for each sample (Dean et al., 2019). We used an age distribution model to estimate the different age contributions to a given mixture for each ^{14}C sample (Dean, van der Velde, et al., 2018; Evans et al., 2014, 2022; Raymond et al., 2007; Tanentzap et al., 2021). This approach assumes that C sources in a given mixture are dominated by C fixed into peat soils in the year prior to sampling, with contributions of exponentially less C from each preceding year up to a maximum peat age of 10,000 years. This model conceptually follows empirical observations of both C accumulation and loss in peatland soils (Ratcliffe et al., 2018) and that discharge contributions to pools in blanket peatlands are mainly generated from near-surface flow paths (Holden et al., 2018). We estimate the age contribution to each ^{14}C mixture (sample) based on reconstructed atmospheric $^{14}CO_2$ which was assumed to be fixed into plant material and formed the organic matter in peat soils each year over the past 10,000 years by solving Equation (1) for λ (the rate parameter, termed "k" in e.g., Evans et al., 2022):

$$F^{14}C_{aq}(t) = \int_0^{inf} \lambda e^{-\lambda T} F^{14}C_{air}(t - T)\, 2^{\frac{T}{5730}}\, dT, \quad (1)$$

where $F^{14}C_{aq}$ is sample ^{14}C content in $F^{14}C$, $F^{14}C_{air}$ is atmospheric ^{14}C-CO_2 content at time (t), and T is the age of the sample in years before sampling date (yBSD). Atmospheric $^{14}CO_2$ was derived from Reimer et al. (2020) for 10,000 years ago to 1950 CE, and from Hua et al. (2022) from 1950 to 2015 CE. These data were then interpolated using a cubic spline (*splinefun* in R) to create a continuous data series. The R script

and associated data files used to analyze and present the data in this study can be found in the associated Github repository (https://github.com/jfdean1/UKpeatlandpool14C). The full atmospheric $^{14}CO_2$ reconstruction is available in the Supporting Information. Analytical uncertainty was propagated through the model by giving an upper and lower bound for each sample (Table S1). We report the median value of the modelled age distribution for each sample:

$$\text{Median Age} = \lambda^{-1} \ln(2). \quad (2)$$

The age distribution modelling and other statistical analyses were carried out in R version 4.1.1 (R Core Team, 2021). To explore differences between the isotopic composition of different C forms and pool locations, we used nonparametric Kruskal–Wallis tests with the *kruskal.test* function in R, supplemented by post hoc analyses consisting of Conover–Iman tests using the *conover.test* function and unpaired two-sample Wilcoxon tests using the *wilcox.test* function. We undertook linear regression analyses using the *lm* function to quantify the relationship between the isotopic composition of DOC, POC, and dissolved CO_2, as well as between DOC and dissolved organic matter (DOM) absorbance parameters where available (Chapman et al., 2022). We used Cook's distance to identify potential outliers in the linear models using the *cooks.distance* function. To explore potential correlations between the isotopic composition of DOC, POC, and dissolved CO_2 and additional biogeochemical parameters available at the Cross Lochs location (collected within ±3 days of the isotope samples; Chapman et al., 2022), we used Spearman's rank correlation in the *rcorr* function. The details of where each analysis is applied are provided in the figure and table captions in the main text and Supporting Information.

We also utilized Keeling and Miller–Tans plots to estimate possible sources for the observed dissolved CO_2 (Campeau, Wallin, et al., 2017). Both approaches assume a mixing of isotopically distinct C sources and conservation of mass (adapted from Campeau, Wallin, et al., 2017):

$$I_{obs} \times C_{obs} = I_s \times C_s + I_b \times C_b, \quad (3)$$

where I_{obs} is the observed sample isotopic composition and C_{obs} is the paired sample CO_2 concentration, which results from a mixture of isotopic composition and CO_2 concentration in a background ($_b$) and a single source ($_s$). The composition of the source can be derived from the *y*-intercept of the simple linear equation in a Keeling plot or the slope of the linear equation in a Miller–Tans plot, assuming linearity in the mixing between two C sources without additional isotopic fractionation.

3 | RESULTS

3.1 | Age and source of carbon in peatland pools

Across six peatland pool locations, we collected 94 aquatic and three sediment ^{14}C samples (Figure 1). Of the aquatic samples,

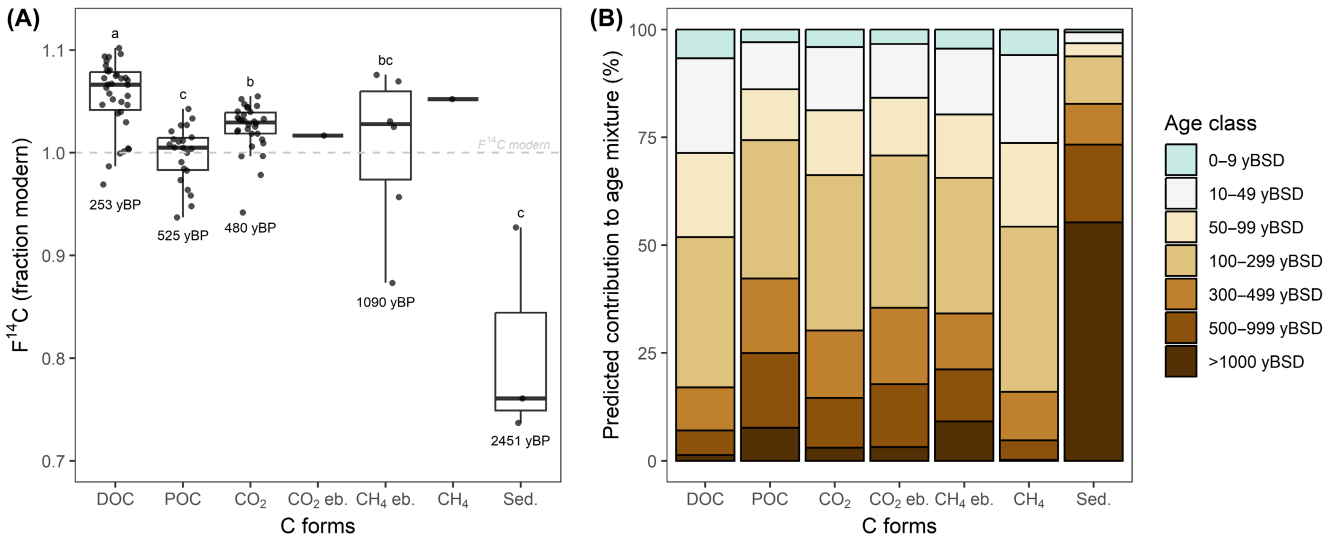

FIGURE 1 Distribution of radiocarbon observations. (A) All radiocarbon observations from this study in fraction modern ($F^{14}C$). Separate boxplots are ordered by C form: DOC ($n = 34$), POC ($n = 22$), dissolved CO_2 ($n = 30$), ebullition (bubble) CO_2 ($n = 1$), dissolved CH_4 ($n = 1$), ebullition CH_4 ($n = 6$), and pool sediments ($n = 3$); thick horizontal lines of the boxes represent medians, limits of the boxes represent upper and lower quartiles, whiskers extend to 1.5 times the interquartile range, dots represent all data points. Lowercase letters indicate statistically significant differences ($p < .05$) between C forms using a Kruskal–Wallis test and Conover–Iman post hoc (excluded where sample $n < 2$); the oldest radiocarbon ages observed for each C species are indicated in years before present (yBP) where "present" = 1950 CE; any data plotting above the dashed horizontal line is considered radiocarbon "modern" (i.e., $F^{14}C > 1$, or younger than 1950 CE). (B) The potential contribution of soil age layers (classes) to the observed mixtures (samples), based on the age distribution model (Tanentzap et al., 2021) and ordered by C form. The relative soil age classes are in years before sampling date (yBSD); $F^{14}C$ analytical uncertainty ($\pm 1\sigma$) was propagated through the age distribution model but is not shown here (Table S1). Only the oldest solutions to the age distribution model are shown (Figure S4). CH_4, methane; CO_2, carbon dioxide; DOC, dissolved organic carbon; POC, particulate organic carbon.

76 (78%) had an $F^{14}C$ content >1, meaning they contain C fixed by primary production since ca. 1955 CE when nuclear testing elevated the ^{14}C content of the atmosphere (Figure S4; Evans et al., 2014). DOC contained more ^{14}C-enriched samples than any other C form (median $F^{14}C$ content = 1.0663, range = 0.9690–1.1019), indicating a generally younger age dominated by bomb-peak C (Figure 1A). Dissolved CO_2 was the next most ^{14}C-enriched (median = 1.0294, range = 0.9420–1.0550), followed by CH_4 ebullition (1.0279, 0.8732–1.0758), and then POC (1.0050, 0.9370–1.0426), with pool sediments containing the lowest ^{14}C content (0.7608, 0.7371–0.9274). Dissolved CO_2 and CH_4 ebullition were statistically alike, as were CH_4 ebullition, POC, and pool sediment. The oldest ^{14}C age of 1090 ± 25 yBP was from ebullition CH_4; although it should be noted that two out of three pool sediment values were noticeably older than the other C forms.

We estimated the potential contribution of different aged peat layers to the C mixtures that make up the $F^{14}C$ observations (Figure 1B; Dean et al., 2019; Tanentzap et al., 2021). DOC likely contains high contributions (~50%) of 0- to 100-year-old C sources, while the other C forms are dominated by contributions of 0- to 300-year-old C (>50%). Organic C as old as 5000 years is common in the upper ~2 m of peat at the study sites (Ratcliffe et al., 2018), but there is no evidence of C this old in the pool waters. Millennial aged C (>1000 years) is likely only present in notable quantities in pool sediments (~50%; Figure 1B) and potentially some POC and ebullition CH_4 (~10%). For each sample, we also estimated its median age in yBSD from the age distributions (Table S1; Dean, van der Velde, et al., 2018). Due to elevated atmospheric $F^{14}C$ levels during the bomb peak, some samples can have median ages either side of this peak (Figure S4; Evans et al., 2014). For example, a dissolved CO_2 sample from pool P07 collected in November 2014 could have a median age of 3 or 133 yBSD (Table S1). We do not attempt to determine if one solution is correct or not, and instead plot all solutions together with the atmospheric $F^{14}C$-CO_2 record to demonstrate that 49 of 94 (52%) of our $F^{14}C$ observations (excluding pool floor sediment) could have both a very young (<10 yBSD) and decadal to centennial (>56 yBSD) median age. These potential young median ages indicate that C in some pools could be almost entirely dominated by primary production in the decade prior to sampling (Figure S4). In Figure 1B, we only show the mean potential contributions of different aged peat layers from the old median ages.

There were some statistically significant differences in $F^{14}C$ between the different peatland pool locations (Figure 2). Garron Plateau had the highest median $F^{14}C$ content (1.0671, range = 1.0326–1.0939), followed by Munsary (1.0696, range = 1.0110–1.0799), Silver Flowe (1.0448, range = 1.0231–1.0660), Slievearnorra (1.0378, range = 1.0305–1.1019), Cross Lochs (1.0218, range = 0.8732–1.0962), and Loch Lier (1.0187, range = 0.9370–1.0807). Garron Plateau and Loch Lier were statistically distinct, while statistical similarities were present between these locations and all others (see lowercase letters denoting statistical significance in Figure 2). This is partly complicated by the

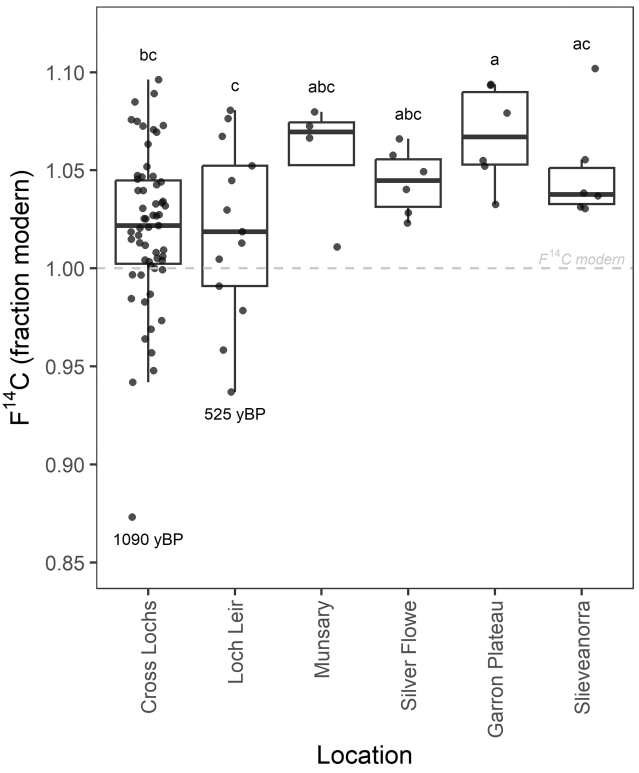

FIGURE 2 All $F^{14}C$ observations across the different peatland pool locations (excluding sediments). Separate boxplots are ordered by location: Cross Lochs ($n = 59$), Loch Leir ($n = 13$), Munsary ($n = 4$), Silver Flowe ($n = 6$), Garron Plateau ($n = 6$), and Slieveanorra ($n = 6$); box features follow Figure 1. Lowercase letters indicate statistically significant differences ($p < .05$) between locations using a Kruskal–Wallis test and Conover–Iman post hoc; the oldest radiocarbon ages observed for each location are indicated in years before present (yBP); any data plotting above the dashed horizontal line are considered radiocarbon "modern."

differing number of samples collected at each site. Cross Lochs was the focus of three sampling campaigns across 2014 and 2015, while the other sites were sampled in single snapshot campaigns. There is also dissimilarity between the number and type of C forms sampled across the sites, which was confounded by logistical challenges in obtaining enough aquatic C for ^{14}C analysis (see Section 2.2; Table S1; Dean et al., 2017). However, we found no notable patterns in the $F^{14}C$ observations due to the timing of the sampling campaigns (Figure S1). Despite the variability in sample number and timing, the $F^{14}C$ observations across 27 pools at six different peatland locations shared several statistical similarities; the majority of samples contained $F^{14}C > 1$, which indicates a predominance of contemporary C fixed post-1950 CE (Figure 2).

3.2 | Comparison of natural and restoration pool types

Overall, there was no significant difference in mean $F^{14}C$ between natural and restoration pools ($p = .3457$; natural $F^{14}C = 1.0268$,

restoration $F^{14}C = 1.0347$; Figure 3A). The $F^{14}C$ content of DOC, however, was significantly different between the two pool types, with more enriched $F^{14}C$-DOC found in the restoration pools (median $F^{14}C = 1.073$, range = 1.0466–1.0962) than natural pools (1.0554, 0.9690–1.1019), which is reflected in the modeled peat layer contributions (Figure 3B). POC (natural = 1.0052, 0.9640–1.0427; restoration = 1.0040, 0.9370–1.0335) and CO_2 (natural = 1.0231, 0.9420–1.0550; restoration = 1.0342, 0.9785–1.0474) were not significantly different between the two pool types (Figure 3).

Isotopic differences between natural and restoration pools were much more pronounced in the $\delta^{13}C$ data (Figure 4). During CO_2 formation, most likely via respiration in these systems, $\delta^{13}C$ is heavily fractionated so the boxplots in Figure 4 are ordered by C form. Across all pools, DOC had a mean $\delta^{13}C$ value of −27.5‰ (range = −29.1‰ to −23.4‰), POC −26.9‰ (−29.9‰ to −24.3‰), and CO_2 −14.4‰ (−20.5‰ to −9.4‰), with DOC and POC values statistically alike. In all C forms, $\delta^{13}C$ was significantly higher (less negative; $p < .05$) in natural pools. Restoration pool DOC had a noticeably smaller range of $\delta^{13}C$ values compared to natural pools and compared to the range of $\delta^{13}C$ values seen in POC and CO_2. Observations of $\delta^{13}C$ come from the same samples as ^{14}C, so face similar problems with consistency in sample collection (see Section 3.1). However, we found no notable patterns in our $\delta^{13}C$ observations due to the timing of the sampling campaigns (Figure S3).

For dissolved CO_2, $F^{14}C$ and $\delta^{13}C$ were significantly related in both natural and restoration pools ($p < .05$; Figure 5C). $F^{14}C$-CO_2 trended from enriched ($F^{14}C > 1$) toward 1 as $\delta^{13}C$-CO_2 trended from −20‰ to −10‰. For DOC and POC, $F^{14}C$ and $\delta^{13}C$ were not related in either pool type (Figure 5A,B). These results suggest that as the main sources of C in dissolved CO_2 trended toward either modern (~2013 CE) or ~1950 CE in age (depending on which side of the ^{14}C bomb peak the samples fall on), the concurrent $\delta^{13}C$ content of dissolved CO_2 became progressively less negative ($\delta^{13}C$-CO_2 produced from organic matter respiration is generally in the −30‰ to −25‰ range; Dean et al., 2020).

3.3 | Relationship between carbon isotopes and other peatland pool parameters

Across all pools where $F^{14}C$ was concurrently measured in DOC and dissolved CO_2, there was a statistically significant linear relationship between the two C forms ($p < .05$; Figure 6A). The statistical significance of this relationship extended to $\delta^{13}C$ across all observations and for restoration pools, but broke down when considering $F^{14}C$ by pool

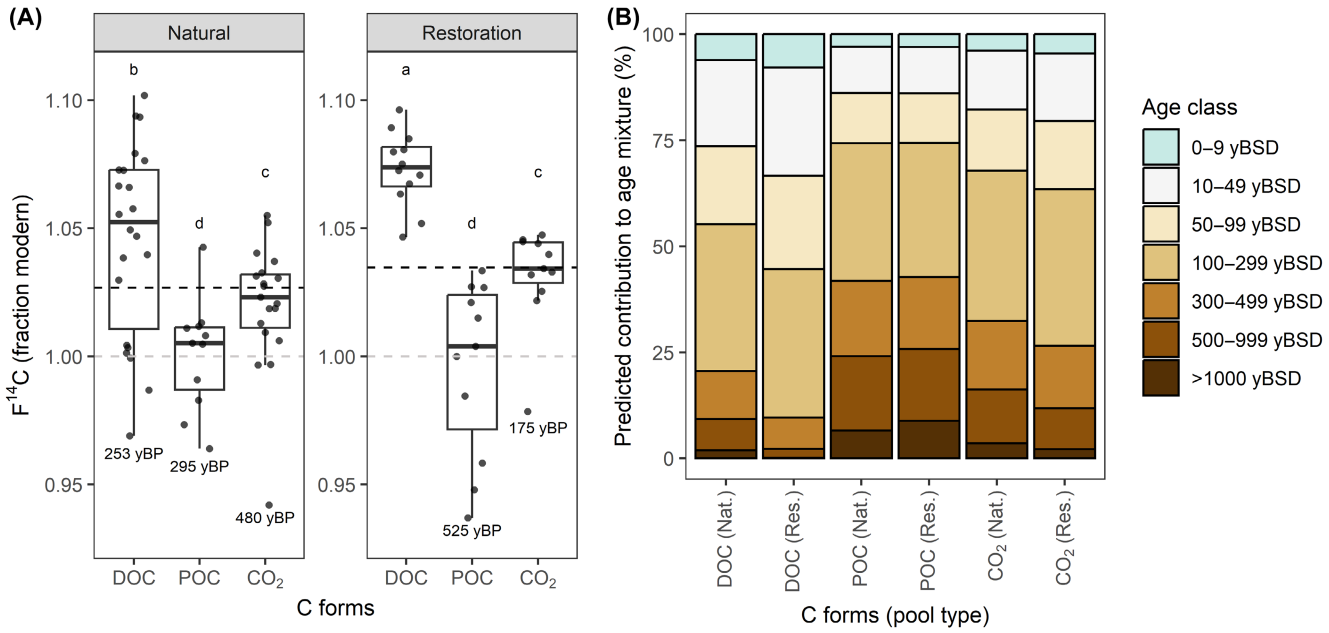

FIGURE 3 Distribution of radiocarbon observations in natural and restoration pool types. (A) $F^{14}C$ observations in the two different pool types sampled in this study (excluding where sample $n < 10$): natural pool DOC ($n = 23$), POC ($n = 11$), and dissolved CO_2 ($n = 19$); restoration pool DOC ($n = 11$), POC ($n = 11$), and dissolved CO_2 ($n = 11$). Box features follow Figure 1; the dashed horizontal lines represent the mean $F^{14}C$ value for each pool type (natural = 1.0268, restoration = 1.0347). Lowercase letters indicate statistically significant differences ($p < .05$) using a series of unpaired two-sample Wilcoxon test by pool type only, and then by C form and pool type (e.g., natural DOC vs. restoration DOC). The oldest radiocarbon ages observed for each C form are indicated in yBP; any data plotting above the dashed horizontal line is considered radiocarbon "modern." (B) The potential contribution of soil age layers (classes) to the observed mixtures (samples), based on the age distribution model (Tanentzap et al., 2021) and ordered by C form and pool type. The relative soil age classes are in yBSD; $F^{14}C$ analytical uncertainty ($\pm 1\sigma$) was propagated through the age distribution model but is not shown here (Table S1). Only the oldest solutions to the age distribution model are shown (Figure S4). CO_2, carbon dioxide; DOC, dissolved organic carbon; POC, particulate organic carbon; yBP, years before present; yBSD, years before sampling date.

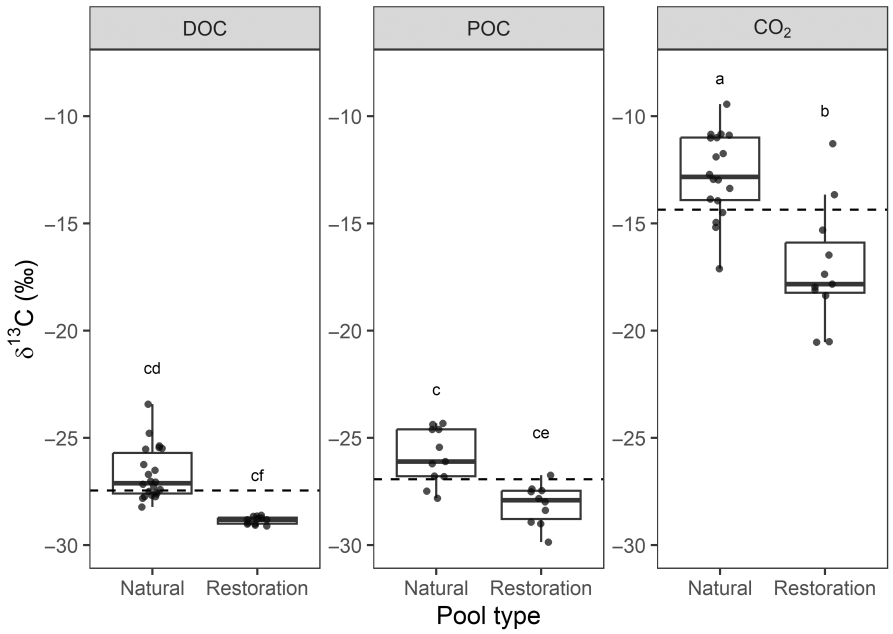

FIGURE 4 Stable C isotope observations ($\delta^{13}C$ in ‰ Vienna Pee Dee Belemnite) in the two pool types measured in this study (excluding where sample $n < 10$): natural pool DOC ($n = 23$), POC ($n = 11$), and dissolved CO_2 ($n = 18$); restoration pool DOC ($n = 11$), POC ($n = 10$), and dissolved CO_2 ($n = 11$). Box features follow Figure 1; the dashed horizontal lines represent the mean $\delta^{13}C$ value for each C form (DOC = −27.56‰, POC = −26.9‰, CO_2 = −14.4‰). Lowercase letters indicate statistically significant differences ($p < .05$) using a Kruskal–Wallis test (C form only) and an unpaired two-sample Wilcoxon test (C form and pool type, e.g., natural DOC vs. restoration DOC). CO_2, carbon dioxide; DOC, dissolved organic carbon; POC, particulate organic carbon.

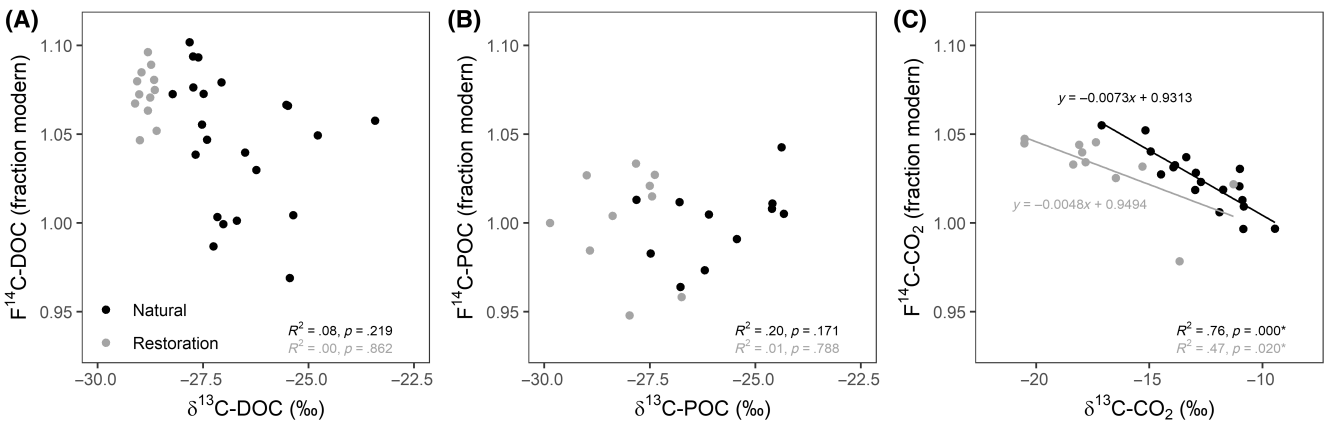

FIGURE 5 $F^{14}C$ versus $\delta^{13}C$ from all sites where paired data were available: DOC (A; $n = 34$), POC (B; $n = 21$), and dissolved CO_2 (C; $n = 29$). Black lines and text represent natural pools, gray lines and text represent restoration pools. R^2-values and p-values are from linear regression; * indicates statistical significance ($p < .05$); lines are only shown for statistically significant relationships. CO_2, carbon dioxide; DOC, dissolved organic carbon; POC, particulate organic carbon.

type and for $\delta^{13}C$ in natural pools (Figure 6B). An unclear relationship was also observed for DOC and POC (Figure 6E,F). $F^{14}C$ in DOC and POC was significantly related only in natural pools, while $\delta^{13}C$ was significantly related across all observations but not when separated by pool type. For dissolved CO_2 and POC, only $\delta^{13}C$ was significantly related and only across all observations, not when separated by pool type (Figure 6C,D). These regressions are likely impacted by the limited sample n when separating the observations by pool type.

For the Cross Lochs pools, we have additional observations of pool biogeochemical parameters from a parallel study (Chapman et al., 2022). We explored possible correlations between our isotopic observations and these additional data were available from concurrent measurement campaigns (campaigns ±3–4 days of each other). These additional parameters were concentrations of DOC, POC, and dissolved CO_2 and CH_4, pH, electrical conductivity, DO, water temperature, and the water table depth in the adjacent peat. $F^{14}C$-DOC and $F^{14}C$-CO_2 were significantly ($p < .05$) correlated with pool DOC concentrations, dissolved CO_2 concentrations, and pH; no other pool biogeochemical parameters were significantly correlated with $F^{14}C$. For $\delta^{13}C$, again the same pool parameters were significantly correlated:

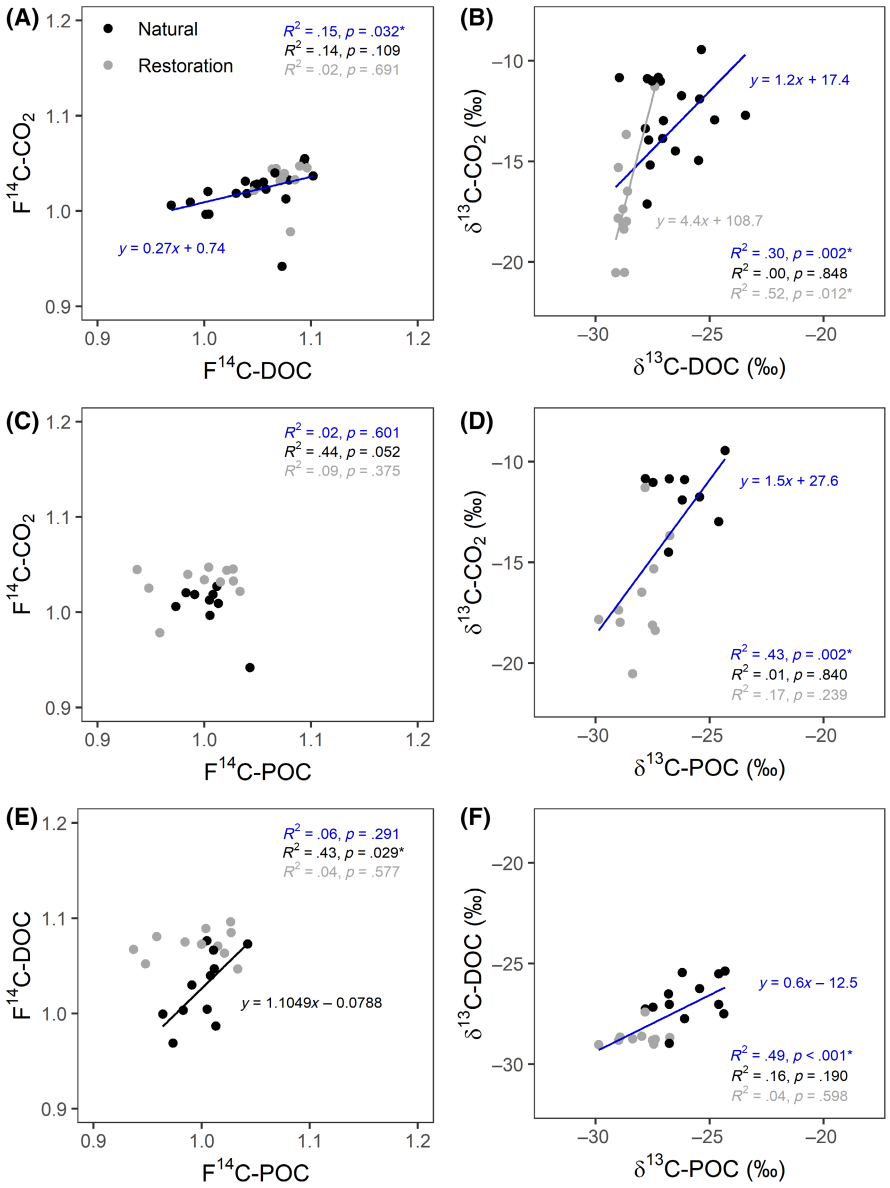

FIGURE 6 Relationship between the isotopic compositions of each carbon form: Fraction modern ($F^{14}C$; A, C, E) and $\delta^{13}C$ (‰ Vienna Pee Dee Belemnite; B, D, F) for paired DOC and CO_2 ($n = 29$), paired CO_2 and POC ($n = 19$), and paired DOC and POC ($n = 22$). Blue lines and text represent combined data for both pool types, black lines and text represent natural pools, gray lines and text represent restoration pools. R^2-values and p-values are from linear regression; * indicates statistical significance ($p < .05$); lines are only shown for statistically significant relationships. CO_2, carbon dioxide; DOC, dissolved organic carbon; POC, particulate organic carbon.

DOC and dissolved CO_2 concentrations, and pH (Table S3). Most of these correlations are impacted by low sample n, skewness in the data and grouping by pool type, which is also evident in Figures 5 and 6 and is primarily driven by differences in $\delta^{13}C$ (Figure 4) rather than $F^{14}C$ (Figure 3). We therefore do not wish to overemphasize the importance of these relationships but present them for completeness.

We additionally looked for relationships between the quality (structure) of DOM in the pools and the DOC isotope observations—unfortunately, due to timing of the parallel sampling campaigns, only data for Cross Lochs in November 2014 and September 2015 were available (Chapman et al., 2022). DOC $F^{14}C$ and $\delta^{13}C$ content were significantly related to SUVA, a proxy for DOM aromaticity (Figure S5; Helms et al., 2008). Neither DOC isotope was significantly related to DOM E4:E6 ratio, a proxy for molecular weight (Helms et al., 2008).

The Keeling and Miller–Tans analyses returned statistically significant linear relationships, despite only being available for a small number of Cross Lochs pools ($n = 17$; Figure S6). For $F^{14}C$, the Keeling regression was statistically significant when considering all samples and for natural pools; the Miller–Tans regression was significant for all samples and when separated by pool type. For $\delta^{13}C$, the Keeling regression was only significant for all samples, not by pool type; the Miller–Tans regression was significant for all samples and when separated by pool type. Combined, these analyses estimated a CO_2 source for all samples with an isotopic composition of −18.6‰ and 1.0427–1.0486 $F^{14}C$. For natural pools, the source isotopic composition estimate was −15.8‰ and 1.0593–1.0767 $F^{14}C$; for restoration pools, the estimate was −18.4‰ and 1.0415 $F^{14}C$.

4 | DISCUSSION

4.1 | Peatland pools dominated by contemporary carbon but old carbon is present in some forms

Our ^{14}C observations across six locations in the United Kingdom indicate that peatland pool C is dominated by contemporary primary

production (Figure 1; Figure S4). The majority of our samples indicate contemporary C mixtures dominated by C younger than 300 yBSD (Figure 1B), and these findings were generally consistent across the broad spatial coverage of the snapshot sampling campaign (Figure 2) and pool type (Figure 3). This finding is surprising given that the top 0.5–1 m of peat surrounding our study pools contains substantial stores of C that is 1000–3000 years old (Ratcliffe et al., 2018), and the pool sediments contained C up to ~2500 years old (Figure 7). Pool location did not have a clear pattern of influence on our $F^{14}C$ observations (Figure 2), meaning the processes discussed hereafter were unlikely to be driven by differences between sampling locations.

That DOC is the youngest C form in these peatland inland water bodies follows previous ^{14}C studies on peatland streams, and rivers globally, where DOC is generally found to be modern (Billett et al., 2007, 2012; Campeau, Bishop, et al., 2017; Dean et al., 2019; Evans et al., 2007, 2022; Marwick et al., 2015; Tipping et al., 2010), except where there is clear disturbance within their catchments (Butman et al., 2015; Hulatt et al., 2014; Moore et al., 2013). DOC-$F^{14}C$ was positively correlated with DOC concentration in the Cross Lochs pools, indicating that increasing DOC concentrations may be driven by contemporary C inputs (Table S3).

Globally, riverine dissolved inorganic C, of which dissolved CO_2 is a constituent, also tends to be modern but can show clear signals of geogenic C release from weathering, including in some United Kingdom peatlands (Billett et al., 2007; Marwick et al., 2015). Our dissolved CO_2 observations are strongly indicative of contemporary primary production, and unlikely to contain inputs from geologic C (Figure 1). Keeling and Miller–Tans plots for our dissolved CO_2 observations from Cross Lochs where CO_2 concentrations were available further indicate a source with a $F^{14}C$ content ranging from 1.0415 to 1.0767 and $\delta^{13}C$ content ranging from −15.8‰ to −18.6‰, neither of which indicate substantial contributions from older peat or geologic C sources (Figure 6). These findings follow previous work on the age of peatland stream dissolved CO_2, which tends to be dominated by contemporary primary production (Campeau, Bishop, et al., 2017; Leith et al., 2014). CO_2-$F^{14}C$ was positively correlated with DOC and CO_2 concentrations, again indicating contemporary C inputs dominate in these pools (Table S3).

POC was older than DOC and CO_2, statistically indistinct from pool sediments, and was estimated to contain 1%–20% C older than 1000 yBSD (Figures 1, 3 and 7). This pattern is reflected in the few studies that have looked at ^{14}C of DOC and POC concurrently in temperate peatland inland waters (Billett et al., 2012), with millennial-aged POC only evident in heavily disturbed catchments (Hulatt et al., 2014). Work in permafrost peatlands also indicates that POC tends to be older than other inland water C forms (Dean et al., 2020). Previous work synthesizing global riverine ^{14}C-POC further suggests the age of POC is correlated with, but generally older than, DOC (Marwick et al., 2015).

Our ebullition data were statistically similar to pool sediments and POC, both of which tended to be older, and dissolved CO_2 which tended to be modern (Figure 1A). We present seven ebullition observations (one CO_2 and six CH_4). Five of our ebullition observations had $F^{14}C$ values >1, indicating a predominance of post-bomb C; two had older ^{14}C ages indicating mixtures dominated by centennial to millennial C; these observations were estimated to contain 0%–35% C older than 1000 yBSD (Figure 1B; Table S1). To our knowledge, these are the first ^{14}C ebullition data for temperate peatland inland waters. In permafrost peatland inland waters, ebullition can be an important pathway for the substantial release of millennial CO_2 and CH_4 (Bouchard et al., 2015; Walter Anthony et al., 2016). Our POC and ebullition observations suggest that millennial C is present in the water column of some peatland pools and can be emitted to the atmosphere.

Although data are limited ($n = 3$), pool floor sediments had the oldest ^{14}C ages in our pools, with ~50% of the C in these samples estimated to be older than 1000 years (Figure 1B). This indicates that there is potential for millennial-aged C input into natural peatland pools possibly via erosion. While older C is unlikely to be contributing to the DOC and CO_2, POC and ebullition CH_4 displayed statistical similarities with these limited sediment data (Figure 1B; Table S1) meaning older C in pool sediments could be contributing to POC or ebullition CH_4.

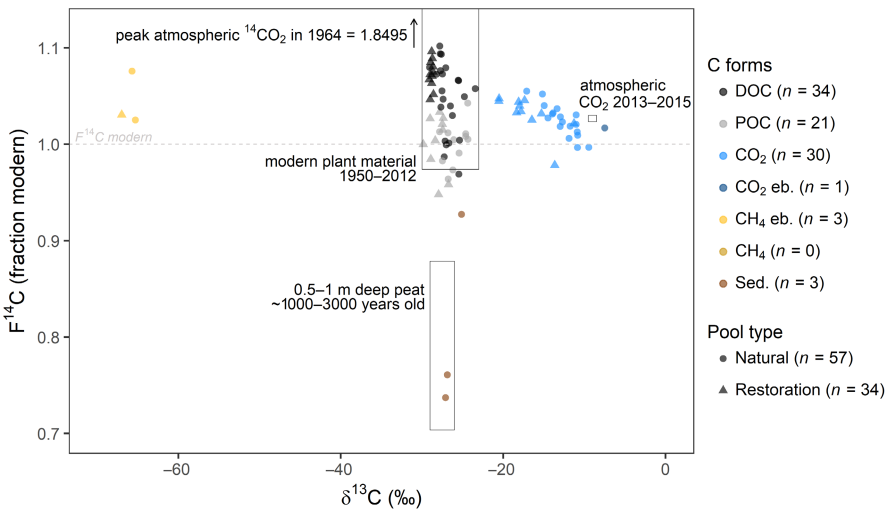

FIGURE 7 Coupled $F^{14}C$ and $\delta^{13}C$ observations for all samples where available (Table S1) and likely C sources. Contemporary (2013–2015) atmospheric $^{14}CO_2$ (Hua et al., 2022), modern (1950–2012) plant material forming the uppermost peat layers (Reimer et al., 2020), and peat in the top 0.5–1 m of the study region (Ratcliffe et al., 2018); $\delta^{13}C$ values are indicative and follow Dean et al. (2020) and Marwick et al. (2015).

4.2 | Limited variability of $F^{14}C$ across pool location and type

No clear pattern emerged when considering all $F^{14}C$ observations by location (Figure 2). The four locations sampled in the wider snapshot campaign that covered only natural pools were all statistically alike (Munsary, Silver Flowe, Garron Plateau and Slieveanorra, sampled in September 2015). There were inconsistent statistical similarities and differences between these four sites and Loch Lier (only sampled once in November 2014 and included natural and restoration pools) and Cross Lochs (sampled in May and November 2014, and September 2015)—these comparisons were hampered by differences in field campaign timing and C form and pool type sampled. For DOC, POC, and dissolved CO_2, which were consistently sampled across both natural and restoration pools, only DOC-$F^{14}C$ was significantly different between the two pool types (Figure 3A). This difference is driven by a likely predominance of younger C in restoration pool DOC relative to the natural pools (Figure 3B).

4.3 | $\delta^{13}C$ content distinctly different between natural and restoration pools, suggesting differences in CO_2 degassing and DOC and POC transformations

Differences between natural and restoration pools were much more pronounced in the $\delta^{13}C$ observations than $F^{14}C$, with $\delta^{13}C$ consistently higher (less negative) and with a greater range in natural pools compared to restoration pools (Figure 4).

For CO_2, the higher $\delta^{13}C$ in natural pools indicates increased mixing with atmospheric CO_2 and/or higher CO_2 co-production with CH_4 relative to restoration pools (Campeau, Wallin, et al., 2017). $F^{14}C$ and $\delta^{13}C$ were significantly related in our CO_2 samples (Figure 5c). This relationship is indicative of pool CO_2 mixing with atmospheric CO_2 (atmospheric CO_2 $F^{14}C = 1.02–1.03$, $\delta^{13}C = -8.5‰$). Assuming the CO_2 isotopic composition we observed is a mixture between atmospheric CO_2 and another source, Keeling and Miller–Tans analyses indicated dissolved CO_2 is primarily derived from a relatively young ($F^{14}C = 1.0415–1.077$) biogenic (−15.8‰ to −18.6‰) source, likely respired modern plant material (Figure 7; Figure S6). These linear models assume that mixing between atmospheric CO_2 and pool CO_2 remains fixed across observations, which is not the case here; furthermore, $\delta^{13}C$ fractionation is known to occur during CO_2 degassing from water. Hence, these source isotopic compositions should be considered estimates.

It is possible that the relationship between CO_2 $F^{14}C$ and $\delta^{13}C$ could instead indicate CO_2 production during methanogenesis if the $F^{14}C$ content of CH_4 in the pools is consistently lower than that of CO_2. We do not have enough concurrent observations of $F^{14}C$-CH_4 to answer this question definitively. A single dissolved CH_4 sample in this study was contemporary (Figure 1A), as were previous $F^{14}C$ observations of restoration pool dissolved CH_4 (Dean et al., 2017), while our ebullition CH_4 observations ranged from contemporary to millennial in age (Figure 1). There was a significant correlation between CO_2 concentration and $\delta^{13}C$-CO_2, suggesting lower concentrations of CO_2 are associated with higher (less negative) $\delta^{13}C$-CO_2 (Table S3). This relationship further supports mixing between pool CO_2 and the atmosphere: $\delta^{13}C$-CO_2 increases with decreasing CO_2 concentrations which indicates mixing with the atmosphere and subsequent degassing. We would expect $\delta^{13}C$-CO_2 to become less negative as CO_2 concentrations increase if this enrichment of $\delta^{13}C$-CO_2 was due to co-production during methanogenesis (Campeau, Wallin, et al., 2017). Concentrations of CO_2 were consistently found to be much lower in natural pools than restoration pools in previous work at the Flow Country sites, which further indicates CO_2 degassing is occurring more readily in natural pools (Chapman et al., 2022). The natural pools tended to be larger in surface area and thus more exposed to wind-driven turbulence that would be higher at the center of wider pools where there is less shelter from the wind, and this turbulence drives atmospheric exchange (Figure S1; Holgerson & Raymond, 2016). Furthermore, Chapman et al. (2022) found a significant linear relationship between CO_2 and CH_4 concentrations in both natural and restoration pools, but the slope of the regression was very shallow suggesting that CO_2 co-production with CH_4 is not the main driver of higher CO_2 concentrations in the pools. We therefore attribute the difference in $\delta^{13}C$-CO_2 between the two pool types to increased exchange with the atmosphere in the natural pools. This demonstrates that natural peatland pools are active sites of CO_2 emission to the atmosphere (Holgerson & Raymond, 2016).

CO_2 dynamics in peatland pools may also be driven by DOC decomposition (Chapman et al., 2022; Pickard et al., 2017). DOC and CO_2 were isotopically coupled when considering all observations together (Figure 6). This isotopic coupling could indicate production of CO_2 from DOC decomposition. Significant correlations were found between both $F^{14}C$-CO_2 and $\delta^{13}C$-CO_2 and DOC concentrations, and between both $F^{14}C$-DOC and $\delta^{13}C$-DOC and CO_2 concentrations, further indicating coupling between DOC and CO_2 dynamics in these pools (Table S3). Previous work at the Flow Country sites found that concentrations of DOC and CO_2 were more strongly related in restoration pools than natural pools (Chapman et al., 2022). When separating our observations by pool type, we only saw a statistically significant relationship between DOC and CO_2 for $\delta^{13}C$ in restoration pools, not in natural pools and not for $F^{14}C$ in either pool type (Figure 6A,B). We also repeated this analysis to remove potential outliers identified using Cook's distance (Figure S7). Repeating these analyses without the six identified potential outliers yielded significant relationships between DOC and CO_2 for $F^{14}C$ overall and when separated by pool type, but did not substantially alter the relationships for $\delta^{13}C$ (Figure 6B; Figure S7). These relationships further indicate that DOC and CO_2 are likely from a similarly aged peat C source, though the $\delta^{13}C$ relationship is complicated by pool CO_2 mixing with the atmosphere (Figure 7).

The wider range of $\delta^{13}C$-DOC values in natural relative to restoration pools (Figure 4) may also indicate increased DOC decomposition occurring within the natural pools. Decomposition can cause fractionation of $\delta^{13}C$, either microbially or through photo-oxidation, although the impact of decomposition on $\delta^{13}C$-DOC in inland

waters is not well characterized (Abbott et al., 2016; Dean, van Hal, et al., 2018; Marwick et al., 2015). Our limited concurrent isotope-DOM structural observations in the Cross Lochs pools indicate that increased DOM decomposition (lower DOM aromaticity as indicated by lower SUVA values) is related to higher (less negative) δ^{13}C-DOC values (Figure S5b). Both relationships seen in Figure S5 could be artifacts of the isotopic differences in DOC between the natural and restoration pools. Regardless, the lower SUVA (aromaticity) values in the natural pools suggest a more decomposed type of DOC resulting in enhanced production of CO_2 (Chapman et al., 2022; Dean et al., 2019; Worrall & Moody, 2014). The natural pools at our sites were generally larger in surface area and had longer water residence times than restoration pools (Figure S1). Larger surface area facilitates increased likelihood of photo-oxidation due to less shading by surrounding vegetation, while longer residence times increases opportunities for DOC decomposition within the pools (Catalán et al., 2016; Chapman et al., 2022).

The lower (more negative) δ^{13}C-POC values in the restoration pools indicate recent POC production from fresh vegetation (Arsenault et al., 2019; Chapman et al., 2022; Dean et al., 2020; Marwick et al., 2015). However, this suggestion is not supported by the F^{14}C-POC data which show that POC is not significantly younger in restoration pools as would be expected if fresh vegetation was the primary source of POC (Figure 3). Furthermore, our POC observations were statistically alike with the pool sediments which contains substantial C older than 1000 years (Figure 1A). Decomposition of POC during residence in the pools, or in the surrounding peat prior to its release into the pool, could explain the differences in δ^{13}C-POC between the two pool types (Attermeyer et al., 2018). POC decomposition could also contribute to CO_2 production as shown by a significant relationship between δ^{13}C in POC and CO_2 (Figure 6d), and a significant correlation between δ^{13}C-POC and CO_2 concentrations (Table S3). Chapman et al. (2022) showed that POC deposition rates were three times higher in natural pools compared to restoration pools, and that DOC may be flocculating to form POC in natural pools. The generally longer water residence times in the restoration pools, and the accompanying decrease in the energy of water flowing through pools, could increase the opportunity for DOC flocculation and POC deposition on pool floors (Figure S1; Chapman et al., 2022). These transformations are likely to impact the isotopic composition of both POC and DOC. DOC and POC F^{14}C were only significantly coupled in natural pools (Figure 6E), while δ^{13}C-POC and DOC concentrations were negatively correlated (Table S3). This could indicate some exchange between DOC and POC, more so in natural pools, such as DOC flocculation to POC (Attermeyer et al., 2018; Dean et al., 2019). For each of DOC and POC individually, F^{14}C and δ^{13}C were not related (Figure 5A,B), suggesting that the differences in DOC and POC decomposition as indicated by δ^{13}C fractionation between the two pool types is not driven by the age (F^{14}C content) of DOC and POC. The limited significant relationships between POC and CO_2 isotopic composition suggest that POC degradation is not a main driver of CO_2 production.

4.4 | Study limitations and future work

Our study provides a unique first insight into peatland pool C age characteristics but remains a "snapshot." From a practical perspective, access could not be afforded by landowners when other priorities of land management took precedence (e.g., sensitive breeding periods and active management interventions). Ideally, further sampling across all seasons and through distinct dry and wet periods should be undertaken to provide further insights into pool C ages and sources. Radiocarbon sampling is challenging in field conditions, particularly for greenhouse gases. Recent technical advances have improved our ability to sample aquatic CO_2 and particularly CH_4 for isotopic analyses, but issues such as low concentrations hampered collection of these samples, including at times DOC and POC during our field campaigns. At Cross Lochs where we sampled consistently during each of the three campaigns, no clear patterns were seen in our isotopic observations due to campaign timing (Figures S2 and S3). No distinct hydrological events were recorded at Cross Lochs prior to or during our field campaigns, with water tables staying within 0–20 cm of the peat surface for the duration of 2014–2015 (Holden et al., 2018). Drain blocking at our study sites occurred more than 10 years ago, meaning that the system has had time to respond to this intervention and potentially even reach an equilibrium state—this could in part explain the similarity of C ages in the two pool types. We thus consider our observations to represent relatively stable conditions at our study sites.

Our observations may not represent the full potential range of environmental conditions at the study sites. The campaigns likely missed periods with the highest temperatures and longest sunlight hours, but did capture the biologically active early summer conditions (May) and periods of relatively low water tables in late summer (September). Warmer and lighter conditions could be a time of increased organic C transformation, such as photo-oxidation, and/or increased inputs from primary production. Our campaigns also do not represent periods of especially large variations in local water tables (Holden et al., 2018). Substantial water table variations can be important for whether shallow younger C or deeper older C is mobilized into inland water systems (Barnes et al., 2018; Chapman et al., 2022). Our campaigns also do not capture diurnal fluctuations, known to be important for the magnitude of inland water greenhouse gas emissions (Attermeyer et al., 2021; Gómez-Gener et al., 2021), nor extreme climatic events such as erosive storm events or long-term drought due to climate change, each of which could significantly alter hydrologic flow paths and C supply to peatland pools.

Therefore, future work could explore the impact of these potential drivers of C supply to the isotopic composition of C mobilized into and emitted from peatland pools. Interesting future work could also consider the evolution of the age of C exported by peatland ditches before, during, and after blocking to determine if, and for how long, the age of aquatic C export changes following restoration efforts. Furthermore, despite the inherent difficulty in collecting reliable ebullition data, further study is warranted as it may be a

potentially important emission pathway of contemporary and old peat C.

5 | CONCLUSIONS

We show that the dominant age (source) of C in pools across a range of peatland locations in the United Kingdom is contemporary primary production. Our limited evidence for the release of old CH_4 via ebullition and the presence of old POC in pool water columns indicates that millennial C can be mobilized in some peatland pools and that these pools are capable of releasing old, previously stored peat C to the atmosphere. Overall, our results indicate that both natural and restoration pools are dominated by contemporary aquatic C. Our analyses identified few significant relationships between peatland pool C isotopes and other pool biogeochemical parameters, although positive correlations between $F^{14}C$ in DOC and CO_2 and DOC and CO_2 concentrations further indicate contemporary C inputs are dominating. We do show that these pools are dynamic, transforming C from one form to another, and releasing some of this C back to the atmosphere, with the generally larger natural pools being more active sites of C transformation and emission. The limited significant relationships between DOC and POC transformations (indicated by $\delta^{13}C$) and $F^{14}C$ suggest the age of the C being transformed is not an important control on the degree to which C decomposition and emission is occurring in these pools. With pools being active sites for the transformation and emission of peatland C, the lack of consistently significant correlations between pool ^{14}C ages and C concentrations also indicates that they remain vulnerable to changes in C inputs from both old and young peat layers driven by peatland disturbance.

Addressing our hypothesis, that peatland pools contain mainly contemporary C but display clear signs of old C release if peatland destabilization is occurring, we observed an overwhelming dominance of contemporary C in most aquatic C forms. Ditch blocking to rewet our study peatlands was effective in preventing the release of old C via aquatic export, as demonstrated by the limited evidence for mobilization of old C. The question remains as to how peatland pool C cycling will respond to substantial influxes of old C from peatland disturbance, and whether restoration pools are as effective in preventing loss of old C in heavily eroding and deeply incised peatlands (Moore et al., 2013; Waldron et al., 2019).

AUTHOR CONTRIBUTIONS

Joshua F. Dean: Data curation; formal analysis; investigation; methodology; validation; visualization; writing – original draft; writing – review and editing. **Michael F. Billett:** Conceptualization; funding acquisition; investigation; methodology; project administration; resources; supervision; validation; visualization; writing – review and editing. **T. Edward Turner:** Formal analysis; investigation; methodology; writing – review and editing. **Mark H. Garnett:** Conceptualization; formal analysis; investigation; methodology; validation; writing – review and editing. **Rebecca M. McKenzie:** Data curation; investigation; methodology; writing – review and editing. **Roxane Andersen:** Conceptualization; data curation; funding acquisition; investigation; methodology; project administration; resources; supervision; visualization; writing – review and editing. **Kerry J. Dinsmore:** Conceptualization; data curation; funding acquisition; investigation; project administration; resources; supervision; writing – review and editing. **Andy J. Baird:** Conceptualization; funding acquisition; investigation; project administration; resources; supervision; visualization; writing – original draft; writing – review and editing. **Pippa J. Chapman:** Conceptualization; data curation; formal analysis; funding acquisition; investigation; methodology; project administration; resources; supervision; visualization; writing – original draft; writing – review and editing. **Joseph Holden:** Conceptualization; data curation; formal analysis; funding acquisition; investigation; methodology; project administration; resources; supervision; visualization; writing – original draft; writing – review and editing.

ACKNOWLEDGMENTS

This work was supported by the United Kingdom Natural Environment Research Council (NERC) grant NE/J007609/1 and NERC Radiocarbon allocation 1832.0514. JFD received additional support from NERC grant NE/V009001/1 and a United Kingdom Research and Innovation Future Leaders Fellowship MR/V025082/1. We are grateful to the Royal Society for the Protection of Birds (RSPB) and Plantlife Scotland for granting and arranging site access, especially Norrie Russell and Daniela Klein of the RSPB for valuable site advice.

CONFLICT OF INTEREST STATEMENT

The authors declare no competing interests.

DATA AVAILABILITY STATEMENT

The underlying isotope data are openly available from the Environmental Information Data Centre (https://doi.org/10.5285/d417b1b9-eaba-4b9d-ba2c-dfb53973b113). Secondary data used from Chapman et al. (2022) are openly available from the Environmental Information Data Centre (https://doi.org/10.5285/17b51437-0231-4eac-a176-1277185ba2e9). The R-code and all additional data used to produce the analyses in this manuscript are openly available via a Github Repository (https://github.com/jfdean1/UKpeatlandpool14C).

ORCID

Joshua F. Dean https://orcid.org/0000-0001-9058-7076
Mark H. Garnett https://orcid.org/0000-0001-6486-2126
Roxane Andersen https://orcid.org/0000-0002-7782-795X
Andy J. Baird https://orcid.org/0000-0001-8198-3229
Pippa J. Chapman https://orcid.org/0000-0003-0438-6855
Joseph Holden https://orcid.org/0000-0002-1108-4831

REFERENCES

Abbott, B. W., Baranov, V., Mendoza-Lera, C., Nikolakopoulou, M., Harjung, A., Kolbe, T., Balasubramanian, M. N., Vaessen, T. N., Ciocca, F., Campeau, A., Wallin, M. B., Romeijn, P., Antonelli, M., Gonçalves, J., Datry, T., Laverman, A. M., de Dreuzy, J.-R., Hannah, D. M., Krause, S., … Pinay, G. (2016). Using multi-tracer inference to move beyond single-catchment ecohydrology. *Earth-Science Reviews*, *160*, 19–42. https://doi.org/10.1016/j.earscirev.2016.06.014

Arsenault, J., Talbot, J., Brown, L. E., Helbig, M., Holden, J., Hoyos-Santillan, J., Jolin, É., Mackenzie, R., Martinez-Cruz, K., Sepulveda-Jauregui, A., & Lapierre, J. (2023). Climate-driven spatial and temporal patterns in peatland pool biogeochemistry. *Global Change Biology*, *29*(14), 4056–4068. https://doi.org/10.1111/gcb.16748

Arsenault, J., Talbot, J., Brown, L. E., Holden, J., Martinez-Cruz, K., Sepulveda-Jauregui, A., Swindles, G. T., Wauthy, M., & Lapierre, J. (2022). Biogeochemical distinctiveness of peatland ponds, thermokarst waterbodies, and lakes. *Geophysical Research Letters*, *49*(11), e2021GL097492. https://doi.org/10.1029/2021GL097492

Arsenault, J., Talbot, J., Moore, T. R., Beauvais, M.-P., Franssen, J., & Roulet, N. T. (2019). The spatial heterogeneity of vegetation, hydrology and water chemistry in a peatland with open-water pools. *Ecosystems*, *22*(6), 1352–1367. https://doi.org/10.1007/s10021-019-00342-4

Attermeyer, K., Casas-Ruiz, J. P., Fuss, T., Pastor, A., Cauvy-Fraunié, S., Sheath, D., Nydahl, A. C., Doretto, A., Portela, A. P., Doyle, B. C., Simov, N., Gutmann Roberts, C., Niedrist, G. H., Timoner, X., Evtimova, V., Barral-Fraga, L., Bašić, T., Audet, J., Deininger, A., … Bodmer, P. (2021). Carbon dioxide fluxes increase from day to night across European streams. *Communications Earth & Environment*, *2*(1), 118. https://doi.org/10.1038/s43247-021-00192-w

Attermeyer, K., Catalán, N., Einarsdottir, K., Freixa, A., Groeneveld, M., Hawkes, J. A., Bergquist, J., & Tranvik, L. J. (2018). Organic carbon processing during transport through boreal inland waters: Particles as important sites. *Journal of Geophysical Research: Biogeosciences*, *123*(8), 2412–2428. https://doi.org/10.1029/2018JG004500

Barnes, R. T., Butman, D. E., Wilson, H. F., & Raymond, P. A. (2018). Riverine export of aged carbon driven by flow path depth and residence time. *Environmental Science & Technology*, *52*(3), 1028–1035. https://doi.org/10.1021/acs.est.7b04717

Billett, M. F., Charman, D. J., Clark, J. M., Evans, C. D., Evans, M. G., Ostle, N. J., Worrall, F., Burden, A., Dinsmore, K. J., Jones, T., McNamara, N. P., Parry, L., Rowson, J. G., & Rose, R. (2010). Carbon balance of UK peatlands: Current state of knowledge and future research challenges. *Climate Research*, *45*(1), 13–29. https://doi.org/10.3354/cr00903

Billett, M. F., Dinsmore, K. J., Smart, R. P., Garnett, M. H., Holden, J., Chapman, P., Baird, A. J., Grayson, R., & Stott, A. W. (2012). Variable source and age of different forms of carbon released from natural peatland pipes. *Journal of Geophysical Research: Biogeosciences*, *117*(2), 1–16. https://doi.org/10.1029/2011JG001807

Billett, M. F., Garnett, M. H., & Harvey, F. (2007). UK peatland streams release old carbon dioxide to the atmosphere and young dissolved organic carbon to rivers. *Geophysical Research Letters*, *34*(23), L23401. https://doi.org/10.1029/2007GL031797

Bouchard, F., Laurion, I., Preskienis, V., Fortier, D., Xu, X., & Whiticar, M. J. (2015). Modern to millennium-old greenhouse gases emitted from ponds and lakes of the Eastern Canadian Arctic (Bylot Island, Nunavut). *Biogeosciences*, *12*(23), 7279–7298. https://doi.org/10.5194/bg-12-7279-2015

Boutton, T. W., Wong, W. W., Hachey, D. L., Lee, L. S., Cabrera, M. P., & Klein, P. D. (1983). Comparison of quartz and pyrex tubes for combustion of organic samples for stable carbon isotope analysis. *Analytical Chemistry*, *55*(11), 1832–1833. https://doi.org/10.1021/ac00261a049

Butman, D. E., Wilson, H. F., Barnes, R. T., Xenopoulos, M. A., & Raymond, P. A. (2015). Increased mobilization of aged carbon to rivers by human disturbance. *Nature Geoscience*, *8*(February), 112–116. https://doi.org/10.1038/NGEO2322

Campeau, A., Bishop, K. H., Billett, M. F., Garnett, M. H., Laudon, H., Leach, J. A., Nilsson, M. B., Öquist, M. G., & Wallin, M. B. (2017). Aquatic export of young dissolved and gaseous carbon from a pristine boreal fen: Implications for peat carbon stock stability. *Global Change Biology*, *23*(12), 5523–5536. https://doi.org/10.1111/gcb.13815

Campeau, A., Wallin, M. B., Giesler, R., Löfgren, S., Mörth, C.-M., Schiff, S., Venkiteswaran, J. J., & Bishop, K. (2017). Multiple sources and sinks of dissolved inorganic carbon across Swedish streams, refocusing the lens of stable C isotopes. *Scientific Reports*, *7*(1), 9158. https://doi.org/10.1038/s41598-017-09049-9

Catalán, N., Marcé, R., Kothawala, D. N., & Tranvik, L. J. (2016). Organic carbon decomposition rates controlled by water retention time across inland waters. *Nature Geoscience*, *9*(7), 501–504. https://doi.org/10.1038/ngeo2720

Chapman, P. J., Moody, C. S., Turner, T. E., McKenzie, R., Dinsmore, K. J., Baird, A. J., Billett, M. F., Andersen, R., Leith, F., & Holden, J. (2022). Carbon concentrations in natural and restoration pools in blanket peatlands. *Hydrological Processes*, *36*(3), e14520. https://doi.org/10.1002/hyp.14520

Dean, J. F., Billett, M. F., Murray, C., & Garnett, M. H. (2017). Ancient dissolved methane in inland waters revealed by a new collection method at low field concentrations for radiocarbon (^{14}C) analysis. *Water Research*, *115*, 236–244. https://doi.org/10.1016/j.watres.2017.03.009

Dean, J. F., Billett, M. F., Turner, T. E., Garnett, M. H., Andersen, R., McKenzie, R. M., Dinsmore, K. J., Baird, A. J., Chapman, P. J., & Holden, J. (2023). *Aquatic carbon isotope composition in natural and restoration pools in blanket peatlands in Scotland and Northern Ireland, 2014-2015*. NERC EDS Environmental Information Data Centre. https://doi.org/10.5285/d417b1b9-eaba-4b9d-ba2c-dfb53973b113

Dean, J. F., Garnett, M. H., Spyrakos, E., & Billett, M. F. (2019). The potential hidden age of dissolved organic carbon exported by peatland streams. *Journal of Geophysical Research: Biogeosciences*, *124*(2), 328–341. https://doi.org/10.1029/2018JG004650

Dean, J. F., Meisel, O. H., Martyn Rosco, M., Marchesini, L. B., Garnett, M. H., Lenderink, H., van Logtestijn, R., Borges, A. V., Bouillon, S., Lambert, T., Röckmann, T., Maximov, T., Petrov, R., Karsanaev, S., Aerts, R., van Huissteden, J., Vonk, J. E., & Dolman, A. J. (2020). East Siberian Arctic inland waters emit mostly contemporary carbon. *Nature Communications*, *11*(1), 1627. https://doi.org/10.1038/s41467-020-15511-6

Dean, J. F., van der Velde, Y., Garnett, M. H., Dinsmore, K. J., Baxter, R., Lessels, J. S., Smith, P., Street, L. E., Subke, J.-A., Tetzlaff, D., Washbourne, I., Wookey, P. A., & Billett, M. F. (2018). Abundant pre-industrial carbon detected in Canadian Arctic headwaters: Implications for the permafrost carbon feedback. *Environmental Research Letters*, *13*(3), 034024. https://doi.org/10.1088/1748-9326/aaa1fe

Dean, J. F., van Hal, J. R., Dolman, A. J., Aerts, R., & Weedon, J. T. (2018). Filtration artefacts in bacterial community composition can affect the outcome of dissolved organic matter biolability assays. *Biogeosciences*, *15*(23), 7141–7154. https://doi.org/10.5194/bg-15-7141-2018

Donahue, D. J., Linick, T. W., & Jull, A. J. T. (1990). Isotope-ratio and background corrections for accelerator mass spectrometry radiocarbon measurements. *Radiocarbon*, *32*(2), 135–142. https://doi.org/10.1017/S0033822200040121

Downing, J. A. (2010). Emerging global role of small lakes and ponds: Little things mean a lot. *Limnetica*, *29*(1), 9–24. https://doi.org/10.23818/limn.29.02

Estop-Aragonés, C., Olefeldt, D., Abbott, B. W., Chanton, J. P., Czimczik, C. I., Dean, J. F., Egan, J. E., Gandois, L., Garnett, M. H., Hartley, I. P., Hoyt, A., Lupascu, M., Natali, S. M., O'Donnell, J. A., Raymond, P. A., Tanentzap, A. J., Tank, S. E., Schuur, E. A. G., Turetsky, M., & Anthony, K. W. (2020). Assessing the potential for mobilization of old soil carbon after permafrost thaw: A synthesis of ^{14}C measurements from the northern permafrost region. *Global Biogeochemical Cycles*, *34*(9), e14520. https://doi.org/10.1029/2020GB006672

Evans, C. D., Freeman, C., Cork, L. G., Thomas, D. N., Reynolds, B., Billett, M. F., Garnett, M. H., & Norris, D. (2007). Evidence against recent climate-induced destabilisation of soil carbon from ^{14}C analysis of riverine dissolved organic matter. *Geophysical Research Letters*, *34*(7), L07407. https://doi.org/10.1029/2007GL029431

Evans, C. D., Page, S. E., Jones, T., Moore, S., Gauci, V., Laiho, R., Hruška, J., Allott, T. E. H., Billett, M. F., Tipping, E., Freeman, C., & Garnett, M. H. (2014). Contrasting vulnerability of drained tropical and high-latitude peatlands to fluvial loss of stored carbon. *Global Biogeochemical Cycles*, *28*(11), 1215–1234. https://doi.org/10.1002/2013GB004782

Evans, C. D., Peacock, M., Baird, A. J., Artz, R. R. E., Burden, A., Callaghan, N., Chapman, P. J., Cooper, H. M., Coyle, M., Craig, E., Cumming, A., Dixon, S., Gauci, V., Grayson, R. P., Helfter, C., Heppell, C. M., Holden, J., Jones, D. L., Kaduk, J., … Morrison, R. (2021). Overriding water table control on managed peatland greenhouse gas emissions. *Nature*, *593*(7860), 548–552. https://doi.org/10.1038/s41586-021-03523-1

Evans, M. G., Alderson, D. M., Evans, C. D., Stimson, A., Allott, T. E. H., Goulsbra, C., Worrall, F., Crouch, T., Walker, J., Garnett, M. H., & Rowson, J. (2022). Carbon loss pathways in degraded peatlands: New insights from radiocarbon measurements of peatland waters. *Journal of Geophysical Research: Biogeosciences*, *127*(7), e2021JG006344. https://doi.org/10.1029/2021JG006344

Friedlingstein, P., O'Sullivan, M., Jones, M. W., Andrew, R. M., Gregor, L., Hauck, J., Le Quéré, C., Luijkx, I. T., Olsen, A., Peters, G. P., Peters, W., Pongratz, J., Schwingshackl, C., Sitch, S., Canadell, J. G., Ciais, P., Jackson, R. B., Alin, S. R., Alkama, R., … Zheng, B. (2022). Global carbon budget 2022. *Earth System Science Data*, *14*(11), 4811–4900. https://doi.org/10.5194/essd-14-4811-2022

Gaffney, P. P. J., Hancock, M. H., Taggart, M. A., & Andersen, R. (2021). Catchment water quality in the year preceding and immediately following restoration of a drained afforested blanket bog. *Biogeochemistry*, *153*(3), 243–262. https://doi.org/10.1007/s10533-021-00782-y

Garnett, M. H., Billett, M. F., Gulliver, P., & Dean, J. F. (2016). A new field approach for the collection of samples for aquatic $^{14}CO_2$ analysis using headspace equilibration and molecular sieve traps: The super headspace method. *Ecohydrology*, *9*(8), 1630–1638. https://doi.org/10.1002/eco.1754

Garnett, M. H., Hardie, S. M. L., & Murray, C. (2011). Radiocarbon and stable carbon analysis of dissolved methane and carbon dioxide from the profile of a raised peat bog. *Radiocarbon*, *53*(1), 71–83. https://doi.org/10.1017/S0033822200034366

Garnett, M. H., Newton, J.-A., & Ascough, P. L. (2019). Advances in the radiocarbon analysis of carbon dioxide at the NERC radiocarbon facility (East Kilbride) using molecular sieve cartridges. *Radiocarbon*, *61*(6), 1855–1865. https://doi.org/10.1017/RDC.2019.86

Gómez-Gener, L., Rocher-Ros, G., Battin, T., Cohen, M. J., Dalmagro, H. J., Dinsmore, K. J., Drake, T. W., Duvert, C., Enrich-Prast, A., Horgby, Å., Johnson, M. S., Kirk, L., Machado-Silva, F., Marzolf, N. S., McDowell, M. J., McDowell, W. H., Miettinen, H., Ojala, A. K., Peter, H., … Sponseller, R. A. (2021). Global carbon dioxide efflux from rivers enhanced by high nocturnal emissions. *Nature Geoscience*, *14*(5), 289–294. https://doi.org/10.1038/s41561-021-00722-3

Gulliksen, S., & Scott, M. (1995). Report of the TIRI workshop, Saturday 13 August 1994. *Radiocarbon*, *37*(2), 820–821. https://doi.org/10.1017/S0033822200031404

Gulliver, P., Waldron, S., Scott, E. M., & Bryant, C. L. (2010). The effect of storage on the radiocarbon, stable carbon and nitrogen isotopic signatures and concentrations of riverine DOM. *Radiocarbon*, *52*(3), 1113–1122. https://doi.org/10.1017/S0033822200046191

Hassan, M., Talbot, J., Arsenault, J., Martinez-Cruz, K., Sepulveda-Jauregui, A., Hoyos-Santillan, J., & Lapierre, J. (2023). Linking dissolved organic matter to CO_2 and CH_4 concentrations in Canadian and Chilean peatland pools. *Global Biogeochemical Cycles*, *37*(4), e2023GB007715. https://doi.org/10.1029/2023GB007715

Helms, J. R., Stubbins, A., Ritchie, J. D., Minor, E. C., Kieber, D. J., & Mopper, K. (2008). Absorption spectral slopes and slope ratios as indicators of molecular weight, source, and photobleaching of chromophoric dissolved organic matter. *Limnology and Oceanography*, *53*(3), 955–969. https://doi.org/10.4319/lo.2008.53.3.0955

Holden, J., Moody, C. S., Edward Turner, T., McKenzie, R., Baird, A. J., Billett, M. F., Chapman, P. J., Dinsmore, K. J., Grayson, R. P., Andersen, R., Gee, C., & Dooling, G. (2018). Water-level dynamics in natural and artificial pools in blanket peatlands. *Hydrological Processes*, *32*(4), 550–561. https://doi.org/10.1002/hyp.11438

Holgerson, M. A., & Raymond, P. A. (2016). Large contribution to inland water CO_2 and CH_4 emissions from very small ponds. *Nature Geoscience*, *9*(3), 222–226. https://doi.org/10.1038/ngeo2654

Hua, Q., Turnbull, J. C., Santos, G. M., Rakowski, A. Z., Ancapichún, S., De Pol-Holz, R., Hammer, S., Lehman, S. J., Levin, I., Miller, J. B., Palmer, J. G., & Turney, C. S. M. (2022). Atmospheric radiocarbon for the period 1950–2019. *Radiocarbon*, *64*(4), 723–745. https://doi.org/10.1017/RDC.2021.95

Hulatt, C. J., Kaartokallio, H., Oinonen, M., Sonninen, E., Stedmon, C. A., & Thomas, D. N. (2014). Radiocarbon dating of fluvial organic matter reveals land-use impacts in boreal peatlands. *Environmental Science & Technology*, *48*(21), 12543–12551. https://doi.org/10.1021/es5030004

Leith, F. I., Garnett, M. H., Dinsmore, K. J., Billett, M. F., & Heal, K. V. (2014). Source and age of dissolved and gaseous carbon in a peatland–riparian–stream continuum: A dual isotope (^{14}C and $\delta^{13}C$) analysis. *Biogeochemistry*, *119*(1–3), 415–433. https://doi.org/10.1007/s10533-014-9977-y

Lupascu, M., Akhtar, H., Smith, T. E. L., & Sukri, R. S. (2020). Post-fire carbon dynamics in the tropical peat swamp forests of Brunei reveal long-term elevated CH_4 flux. *Global Change Biology*, *26*(9), 5125–5145. https://doi.org/10.1111/gcb.15195

Marwick, T. R., Tamooh, F., Teodoru, C. R., Borges, A. V., Darchambeau, F., & Bouillon, S. (2015). The age of river-transported carbon: A global perspective. *Global Biogeochemical Cycles*, *29*(2), 122–137. https://doi.org/10.1002/2014GB004911

Moore, S., Evans, C. D., Page, S. E., Garnett, M. H., Jones, T. G., Freeman, C., Hooijer, A., Wiltshire, A. J., Limin, S. H., & Gauci, V. (2013). Deep instability of deforested tropical peatlands revealed by fluvial organic carbon fluxes. *Nature*, *493*(7434), 660–663. https://doi.org/10.1038/nature11818

Page, S., Mishra, S., Agus, F., Anshari, G., Dargie, G., Evers, S., Jauhiainen, J., Jaya, A., Jovani-Sancho, A. J., Laurén, A., Sjögersten, S., Suspense, I. A., Wijedasa, L. S., & Evans, C. D. (2022). Anthropogenic impacts on lowland tropical peatland biogeochemistry. *Nature Reviews Earth & Environment*, *3*(7), 426–443. https://doi.org/10.1038/s43017-022-00289-6

Parry, L. E., Holden, J., & Chapman, P. J. (2014). Restoration of blanket peatlands. *Journal of Environmental Management*, *133*, 193–205. https://doi.org/10.1016/j.jenvman.2013.11.033

Peacock, M., Audet, J., Bastviken, D., Cook, S., Evans, C. D., Grinham, A., Holgerson, M. A., Högbom, L., Pickard, A. E., Zieliński, P., & Futter, M. N. (2021). Small artificial waterbodies are widespread and persistent emitters of methane and carbon dioxide. *Global Change Biology*, *27*(20), 5109–5123. https://doi.org/10.1111/gcb.15762

Pickard, A. E., Heal, K. V., McLeod, A. R., & Dinsmore, K. J. (2017). Temporal changes in photoreactivity of dissolved organic carbon and implications for aquatic carbon fluxes from peatlands. *Biogeosciences*, *14*(7), 1793–1809. https://doi.org/10.5194/bg-14-1793-2017

Prėskienis, V., Laurion, I., Bouchard, F., Douglas, P. M. J., Billett, M. F., Fortier, D., & Xu, X. (2021). Seasonal patterns in greenhouse gas emissions from lakes and ponds in a high Arctic polygonal landscape. *Limnology and Oceanography*, *66*(S1), S117–S141. https://doi.org/10.1002/lno.11660

Putra, S. S., Holden, J., & Baird, A. J. (2021). The effects of ditch dams on water-level dynamics in tropical peatlands. *Hydrological Processes*, *35*(5), e14174. https://doi.org/10.1002/hyp.14174

R Core Team. (2021). *R: A language and environment for statistical computing*. R Foundation for Statistical Computing. https://www.R-project.org/

Ratcliffe, J., Andersen, R., Anderson, R., Newton, A., Campbell, D., Mauquoy, D., & Payne, R. (2018). Contemporary carbon fluxes do not reflect the long-term carbon balance for an Atlantic blanket bog. *The Holocene*, *28*(1), 140–149. https://doi.org/10.1177/0959683617715689

Raymond, P. A., McClelland, J. W., Holmes, R. M., Zhulidov, A. V., Mull, K., Peterson, B. J., Striegl, R. G., Aiken, G. R., & Gurtovaya, T. Y. (2007). Flux and age of dissolved organic carbon exported to the Arctic Ocean: A carbon isotopic study of the five largest arctic rivers. *Global Biogeochemical Cycles*, *21*(4), GB4011. https://doi.org/10.1029/2007GB002934

Reimer, P. J., Austin, W. E. N., Bard, E., Bayliss, A., Blackwell, P. G., Bronk Ramsey, C., Butzin, M., Cheng, H., Edwards, R. L., Friedrich, M., Grootes, P. M., Guilderson, T. P., Hajdas, I., Heaton, T. J., Hogg, A. G., Hughen, K. A., Kromer, B., Manning, S. W., Muscheler, R., … Talamo, S. (2020). The IntCal20 Northern Hemisphere radiocarbon age calibration curve (0–55 cal kBP). *Radiocarbon*, *62*(4), 725–757. https://doi.org/10.1017/RDC.2020.41

Rosentreter, J. A., Borges, A. V., Deemer, B. R., Holgerson, M. A., Liu, S., Song, C., Melack, J., Raymond, P. A., Duarte, C. M., Allen, G. H., Olefeldt, D., Poulter, B., Battin, T. I., & Eyre, B. D. (2021). Half of global methane emissions come from highly variable aquatic ecosystem sources. *Nature Geoscience*, *14*(4), 225–230. https://doi.org/10.1038/s41561-021-00715-2

Schwab, M. S., Hilton, R. G., Raymond, P. A., Haghipour, N., Amos, E., Tank, S. E., Holmes, R. M., Tipper, E. T., & Eglinton, T. I. (2020). An abrupt aging of dissolved organic carbon in large Arctic rivers. *Geophysical Research Letters*, *47*(23), e2020GL088823. https://doi.org/10.1029/2020GL088823

Stuart, J. E. M., Tucker, C. L., Lilleskov, E. A., Kolka, R. K., Chimner, R. A., Heckman, K. A., & Kane, E. S. (2023). Evidence for older carbon loss with lowered water tables and changing plant functional groups in peatlands. *Global Change Biology*, *29*(3), 780–793. https://doi.org/10.1111/gcb.16508

Stuiver, M., & Polach, H. A. (1977). Discussion reporting of ^{14}C data. *Radiocarbon*, *19*(3), 355–363. https://doi.org/10.1017/S0033822200003672

Tanentzap, A. J., Burd, K., Kuhn, M., Estop-Aragonés, C., Tank, S. E., & Olefeldt, D. (2021). Aged soils contribute little to contemporary carbon cycling downstream of thawing permafrost peatlands. *Global Change Biology*, *27*(20), 5368–5382. https://doi.org/10.1111/gcb.15756

Tipping, E., Billett, M. F., Bryant, C. L., Buckingham, S., & Thacker, S. A. (2010). Sources and ages of dissolved organic matter in peatland streams: Evidence from chemistry mixture modelling and radiocarbon data. *Biogeochemistry*, *100*(1–3), 121–137. https://doi.org/10.1007/s10533-010-9409-6

Turner, T. E., Billett, M. F., Baird, A. J., Chapman, P. J., Dinsmore, K. J., & Holden, J. (2016). Regional variation in the biogeochemical and physical characteristics of natural peatland pools. *Science of the Total Environment*, *545–546*, 84–94. https://doi.org/10.1016/j.scitotenv.2015.12.101

Waldron, S., Vihermaa, L., Evers, S., Garnett, M. H., Newton, J., & Henderson, A. C. G. (2019). C mobilisation in disturbed tropical peat swamps: Old DOC can fuel the fluvial efflux of old carbon dioxide, but site recovery can occur. *Scientific Reports*, *9*(1), 11429. https://doi.org/10.1038/s41598-019-46534-9

Walter Anthony, K., Daanen, R., Anthony, P., Schneider von Deimling, T., Ping, C.-L., Chanton, J. P., & Grosse, G. (2016). Methane emissions proportional to permafrost carbon thawed in Arctic lakes since the 1950s. *Nature Geoscience*, *9*(9), 679–682. https://doi.org/10.1038/ngeo2795

Worrall, F., & Moody, C. S. (2014). Modeling the rate of turnover of DOC and particulate organic carbon in a UK, peat-hosted stream: Including diurnal cycling in short-residence time systems. *Journal of Geophysical Research: Biogeosciences*, *119*(10), 1934–1946. https://doi.org/10.1002/2014JG002671

Xu, J., Morris, P. J., Liu, J., & Holden, J. (2018). PEATMAP: Refining estimates of global peatland distribution based on a meta-analysis. *Catena*, *160*, 134–140. https://doi.org/10.1016/j.catena.2017.09.010

Xu, S., Anderson, R., Bryant, C., Cook, G. T., Dougans, A., Freeman, S., Naysmith, P., Schnabel, C., & Scott, E. M. (2004). Capabilities of the new SUERC 5MV AMS facility for ^{14}C dating. *Radiocarbon*, *46*(1), 59–64. https://doi.org/10.1017/S0033822200039357

SUPPORTING INFORMATION

Additional supporting information can be found online in the Supporting Information section at the end of this article.

How to cite this article: Dean, J. F., Billett, M. F., Turner, T. E., Garnett, M. H., Andersen, R., McKenzie, R. M., Dinsmore, K. J., Baird, A. J., Chapman, P. J., & Holden, J. (2023). Peatland pools are tightly coupled to the contemporary carbon cycle. *Global Change Biology*, *30*, e16999. https://doi.org/10.1111/gcb.16999